FIG.1A

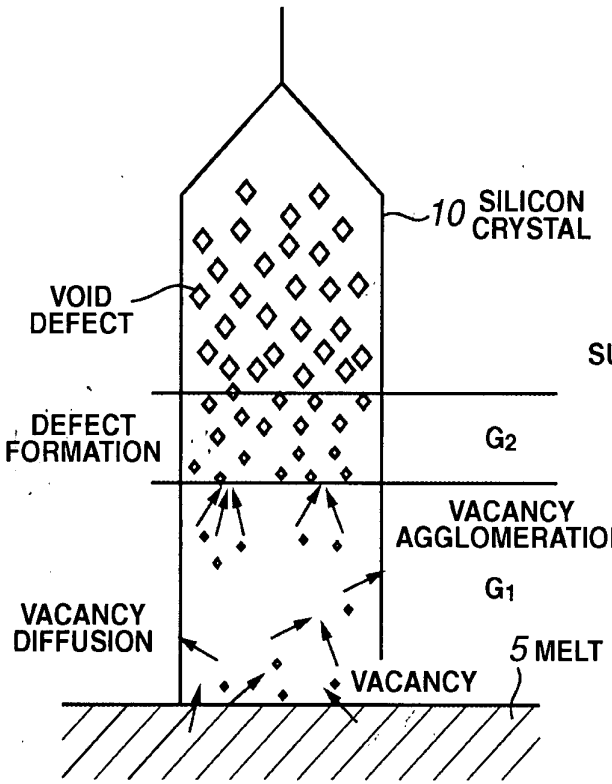

FIG.1B

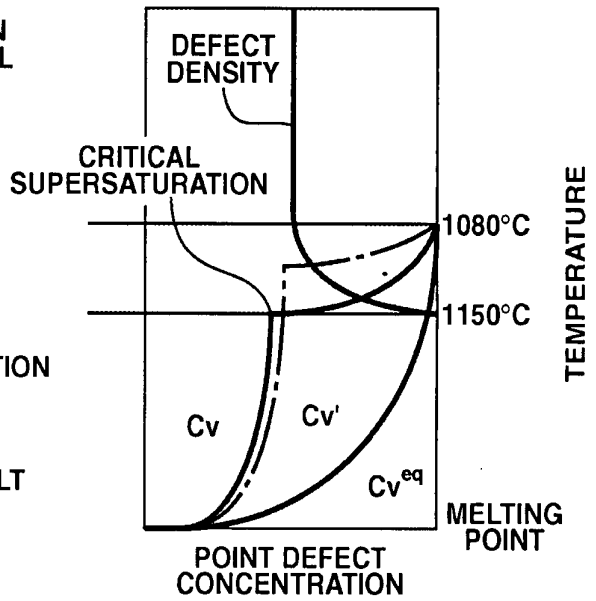

CONCEPTUAL DIAGRAM OF DEFECT FORMATION MECHANISM

FIG.2

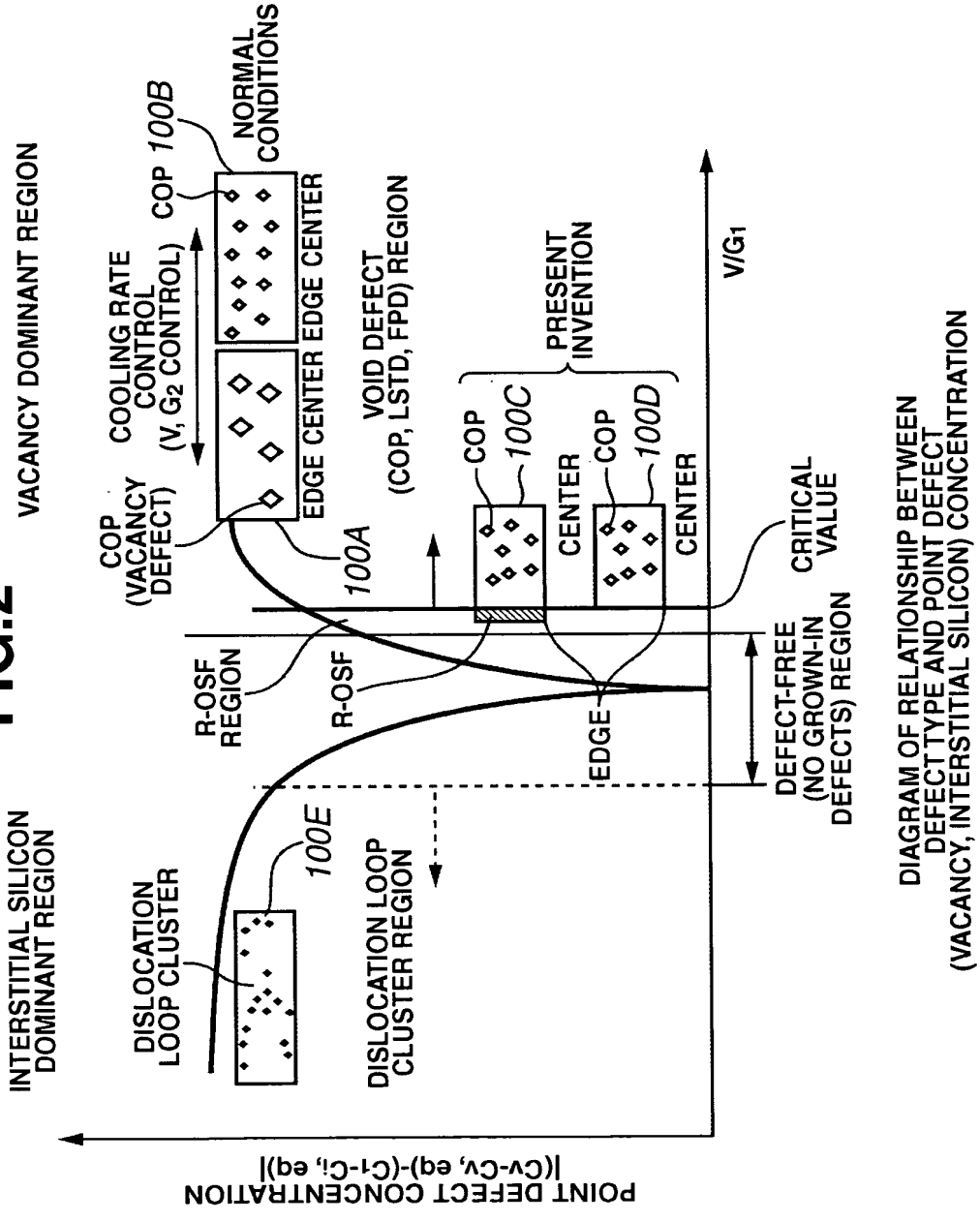
VACANCY DOMINANT REGION
INTERSTITIAL SILICON DOMINANT REGION
POINT DEFECT CONCENTRATION |(Cv-Cv, eq)-(Ci-Ci, eq)|
V/G1
CRITICAL VALUE
NORMAL CONDITIONS
COP 100B
COOLING RATE CONTROL (V, G2 CONTROL)
COP (VACANCY DEFECT)
EDGE CENTER EDGE CENTER
100A
VOID DEFECT (COP, LSTD, FPD) REGION
PRESENT INVENTION
COP 100C
COP 100D
CENTER
CENTER
R-OSF REGION
R-OSF
EDGE
DEFECT-FREE (NO GROWN-IN DEFECTS) REGION
DISLOCATION LOOP CLUSTER
100E
DISLOCATION LOOP CLUSTER REGION
DIAGRAM OF RELATIONSHIP BETWEEN DEFECT TYPE AND POINT DEFECT (VACANCY, INTERSTITIAL SILICON) CONCENTRATION

FIG.3

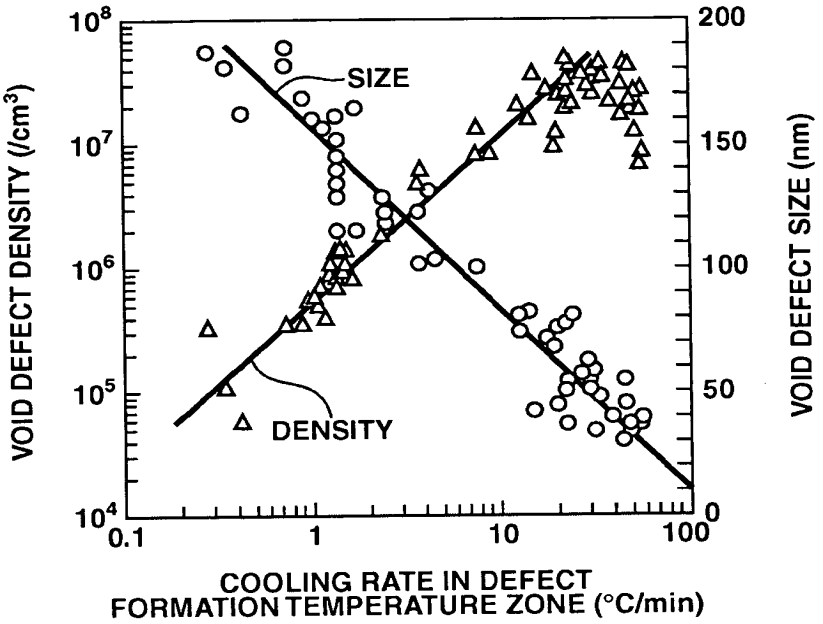

RELATIONSHIP BETWEEN COOLING RATE AND VOID DEFECT DENSITY AND SIZE

FIG.4

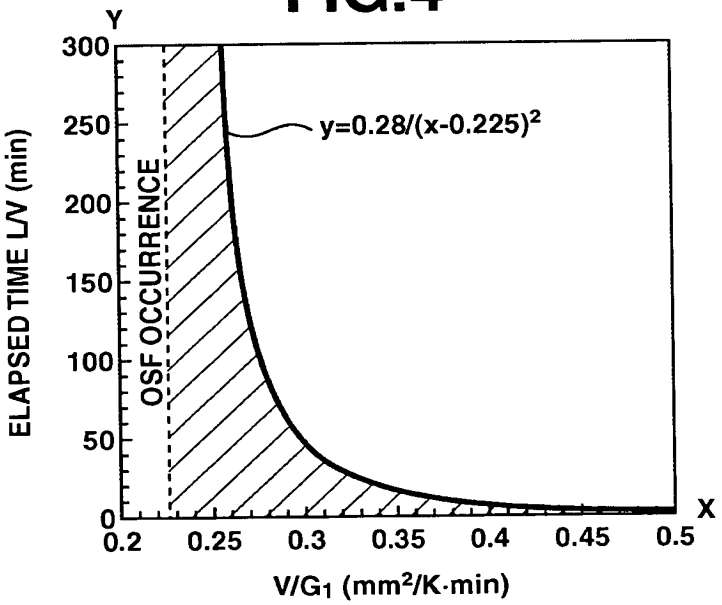

RELATIONSHIP BETWEEN V/G_1 AND ELAPSED TIME (PRIOR ART)

FIG.5

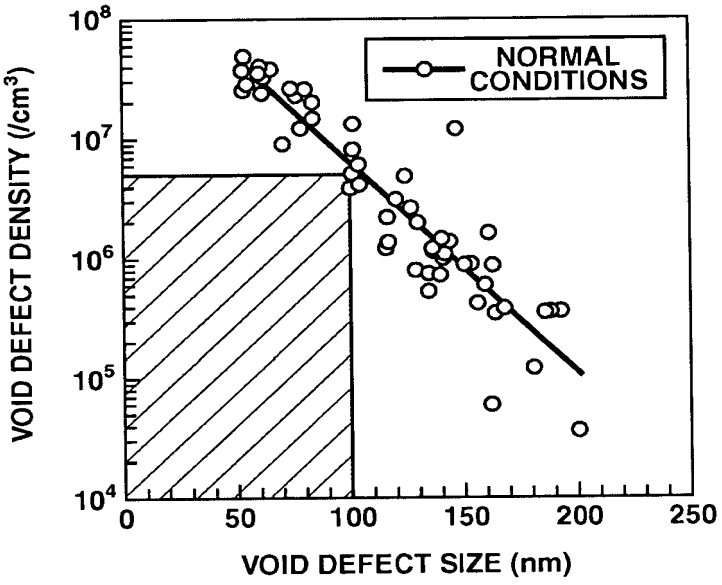

RELATIONSHIP BETWEEN VOID DEFECT DENSITY AND VOID DEFECT SIZE

FIG.6

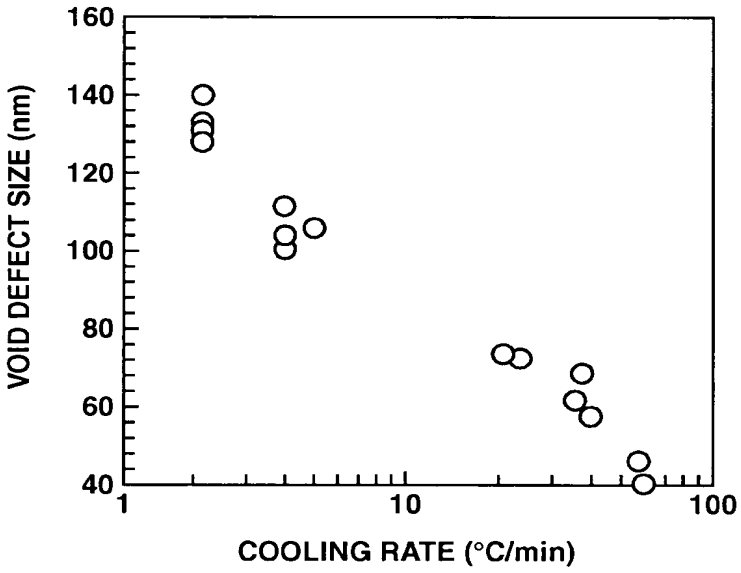

RELATIONSHIP BETWEEN COOLING RATE AT 1100°C AND VOID DEFECT SIZE (WHEN V/G_1 IS AT LEAST ABOUT TWO TIMES THE CRITICAL VALUE)

FIG.7A

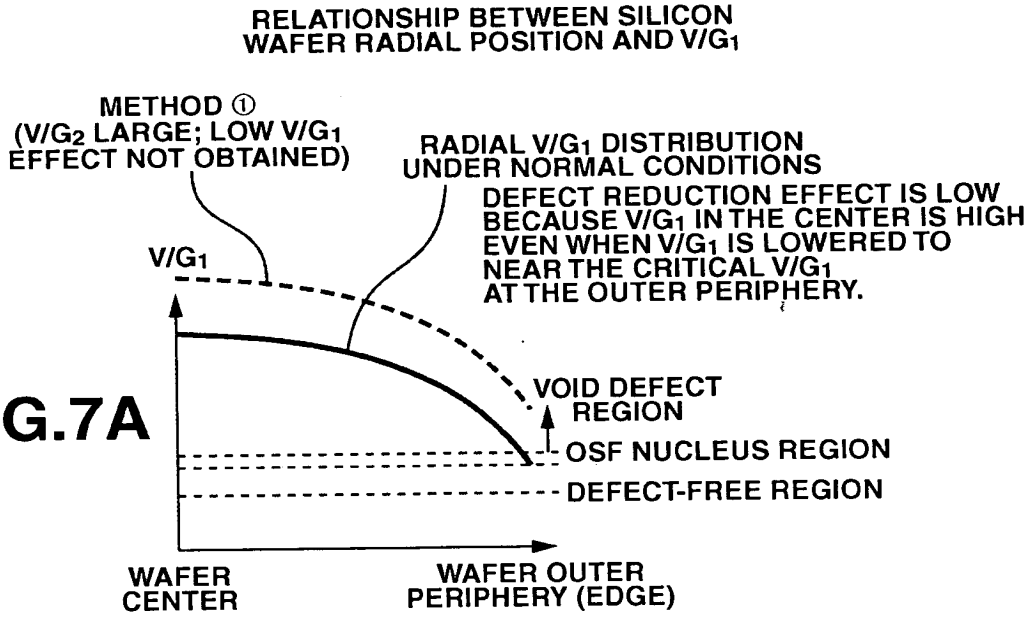

FIG.7B

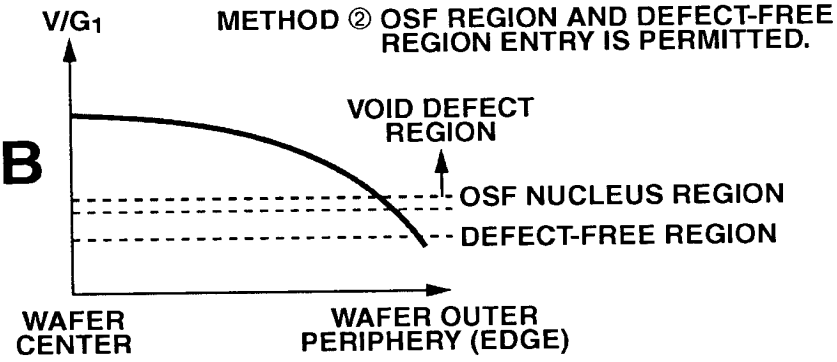

FIG.7C

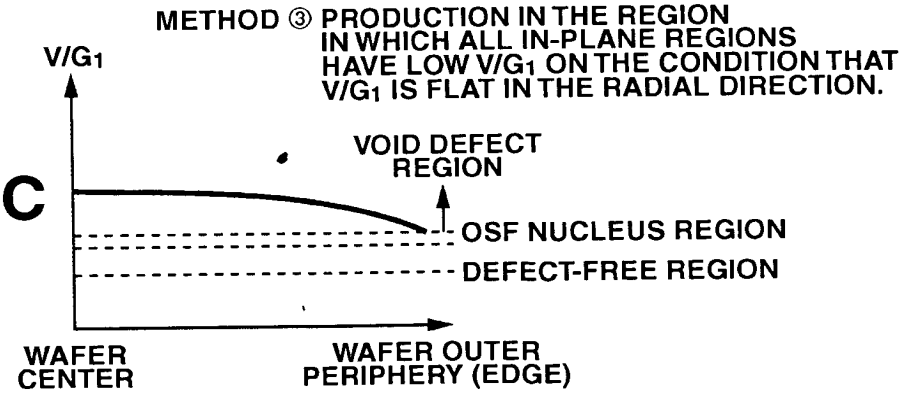

FIG.8

RELATIONSHIP BETWEEN PULLING RATE, SOLID-LIQUID INTERFACE SHAPE, AND OSF OCCURRENCE PULLING RATE UNDER NORMAL CONDITIONS

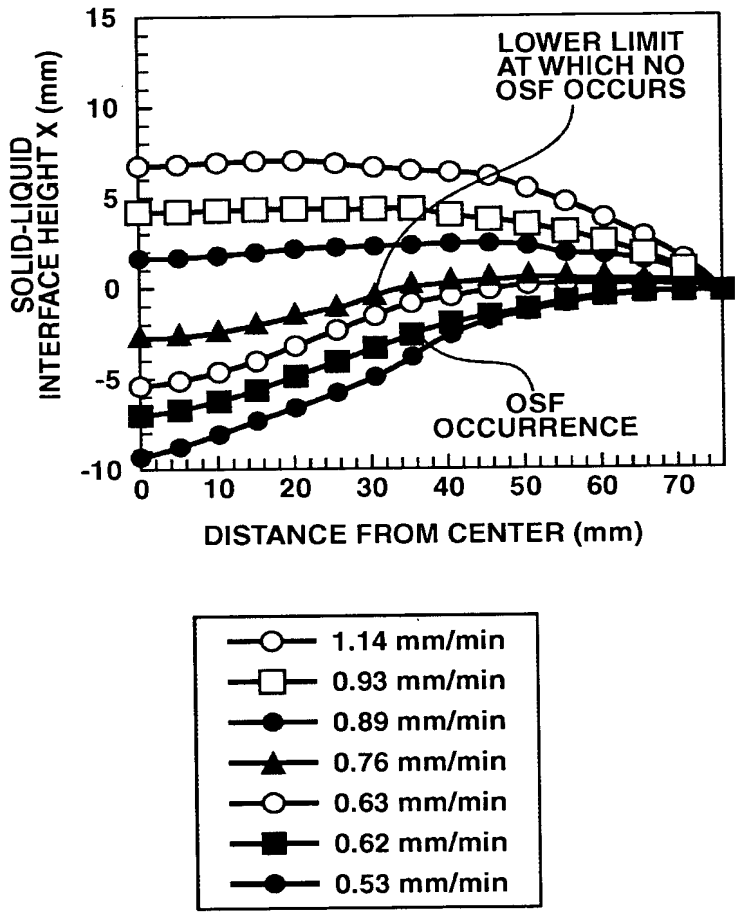

FIG.9

RELATIONSHIP BETWEEN PULLING RATE, SOLID-LIQUID INTERFACE SHAPE, AND OSF OCCURRENCE PULLING RATE UNDER CONDITION OF APPLICATION OF 3000 G HORIZONTAL MAGNETIC FIELD

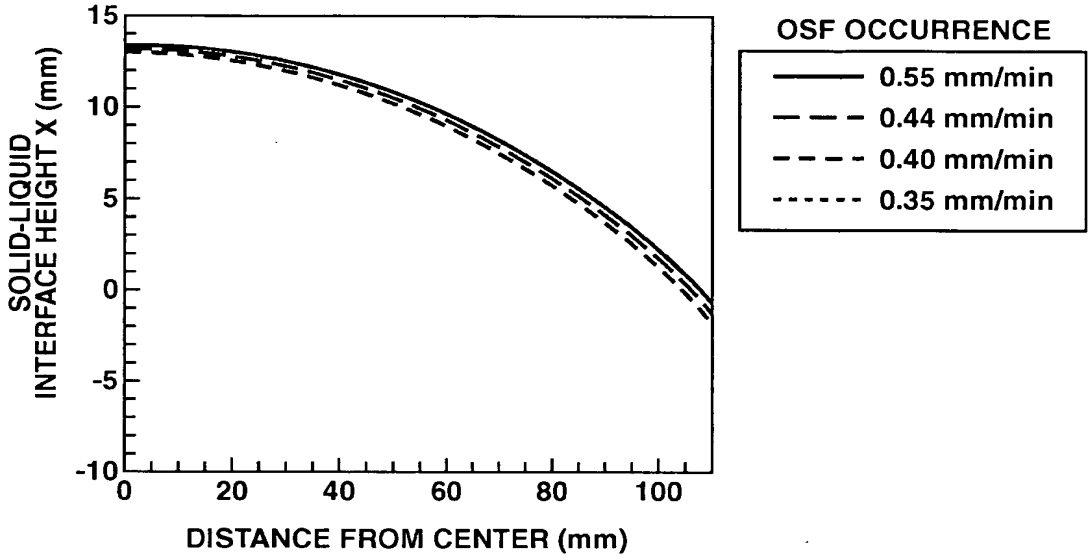

FIG.10

RELATIONSHIP BETWEEN PULLING RATE, SOLID-LIQUID INTERFACE SHAPE, AND OSF OCCURRENCE PULLING RATE UNDER CONDITION OF COOLER INSTALLATION

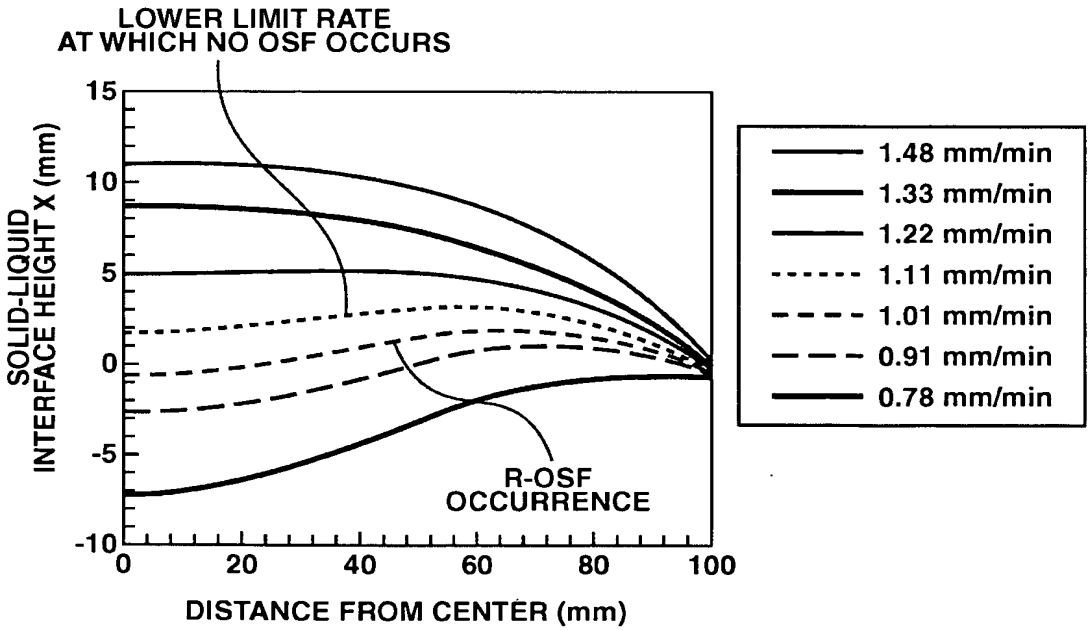

FIG.11

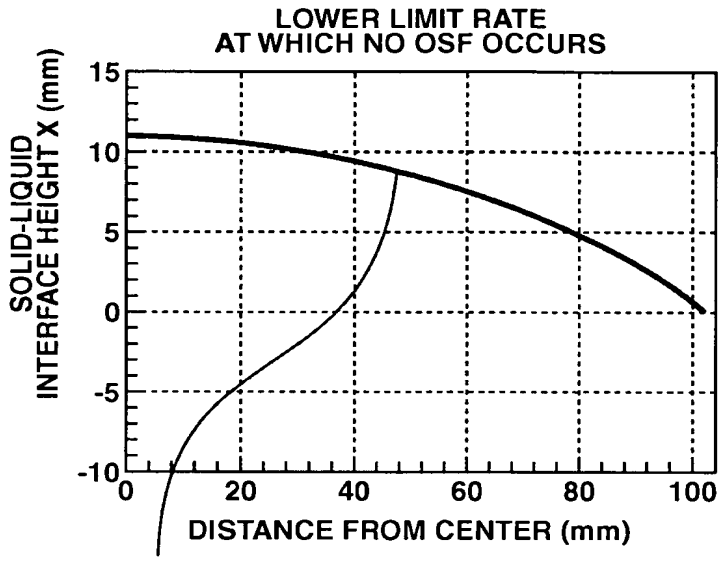

FIG.12

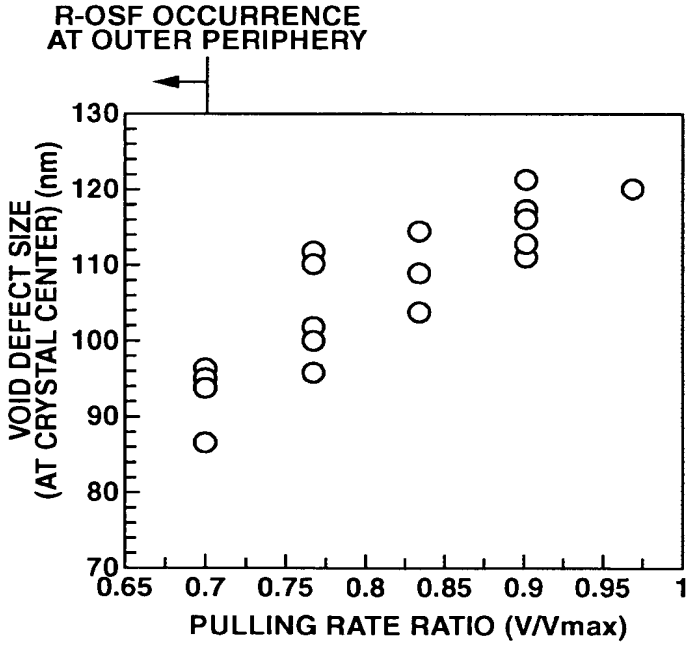

RELATIONSHIP BETWEEN VOID DEFECT SIZE
AT CENTER OF CRYSTAL AND PULLING RATE RATIO
UNDER CONDITION OF COOLER INSTALLATION

RELATIONSHIP BETWEEN PULLING RATE AND VOID DEFECT SIZE AT CRYSTAL CENTER

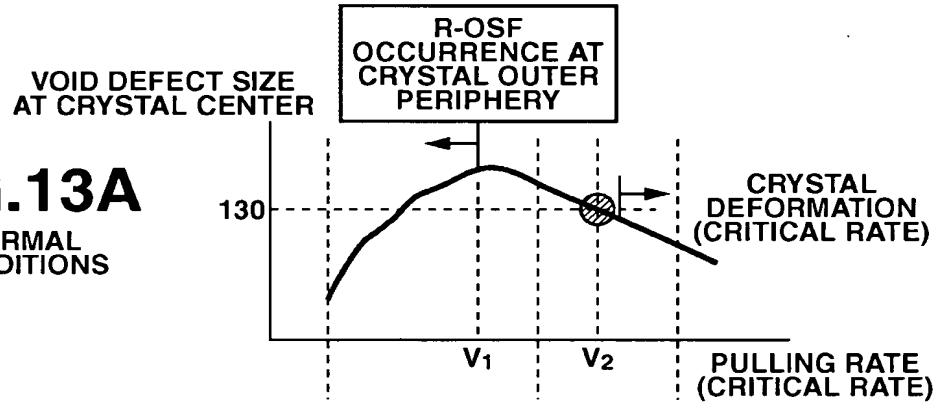

FIG.13A
NORMAL CONDITIONS

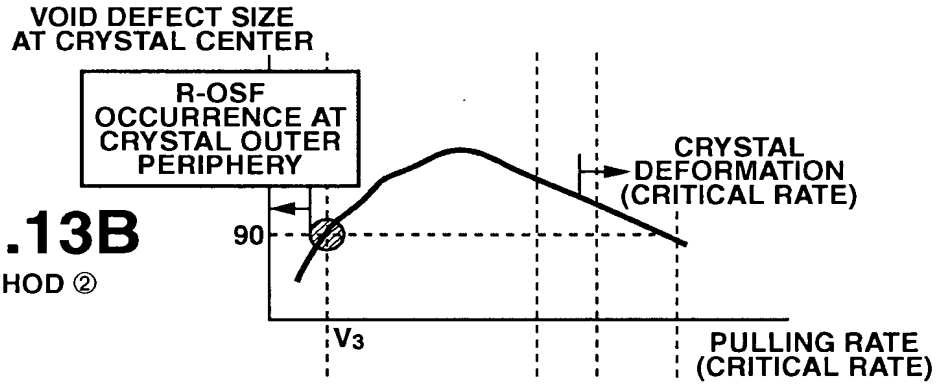

FIG.13B
METHOD ②

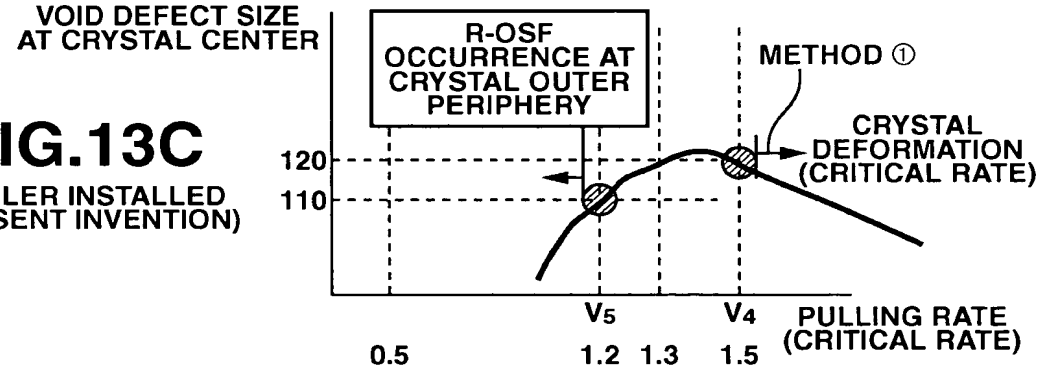

FIG.13C
COOLER INSTALLED (PRESENT INVENTION)

CORRESPONDENCE AMONG PULLING RATE RATIO, PRESENCE OR ABSENCE OF OSF REGION, AND HISTOGRAMS OF LPD COUNT PER WAFER UNDER CONDITION OF COOLER INSTALLATION

	PULLING RATE (mm/min)	PULLING RATE RATIO (V/Vmax)	PRESENCE OR ABSENCE OF WAFER IN-PLANE R-OSF REGION	
FIG.14A	1.45	0.97	ABSENT	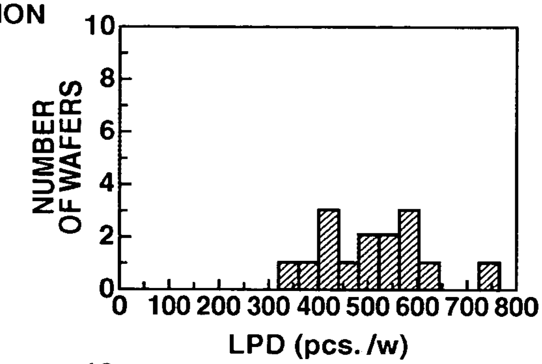
FIG.14B	1.25	0.83	ABSENT	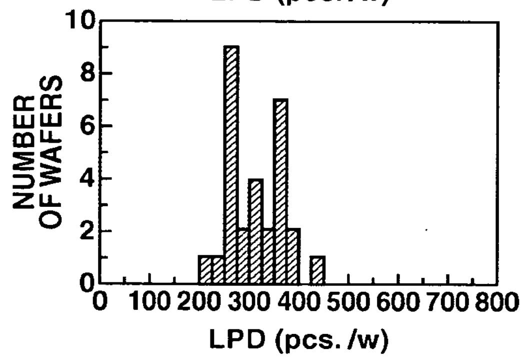
FIG.14C	1.15	0.77	ABSENT	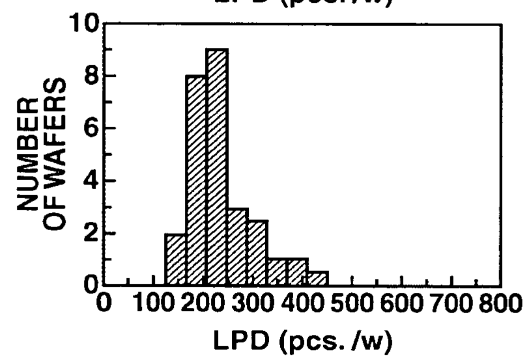
FIG.14D	1.05	0.70	PRESENT	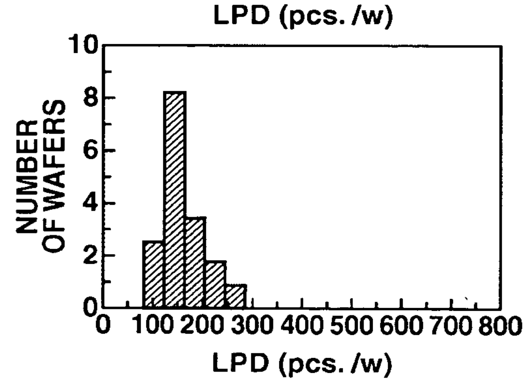

FIG.15

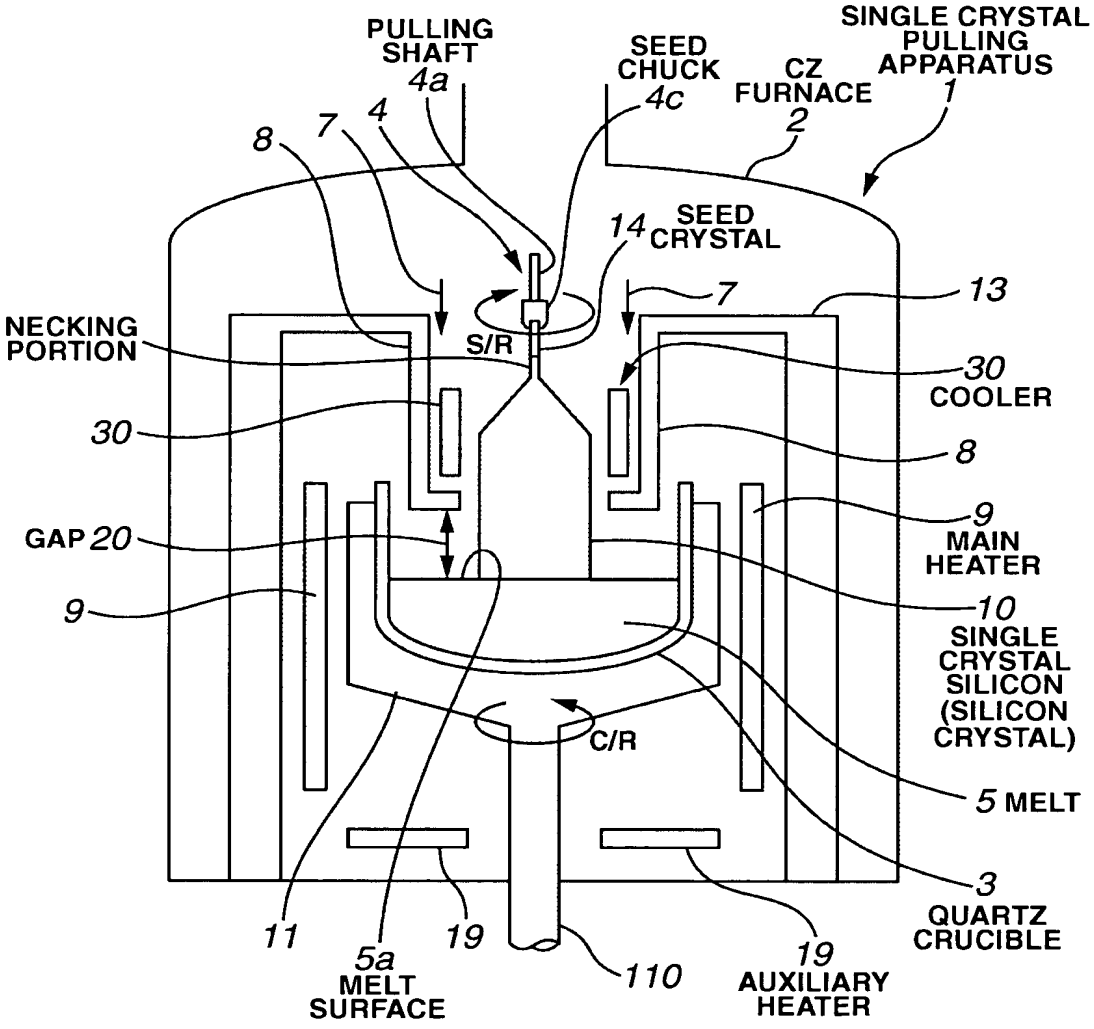

4 PULLING MECHANISM
4a PULLING SHAFT
7 ARGON GAS
8 HEAT BLOCKING PLATE
10 ROTARY SHAFT
11 GRAPHITE CRUCIBLE
13 INSULATING CYLINDER

FIG.16

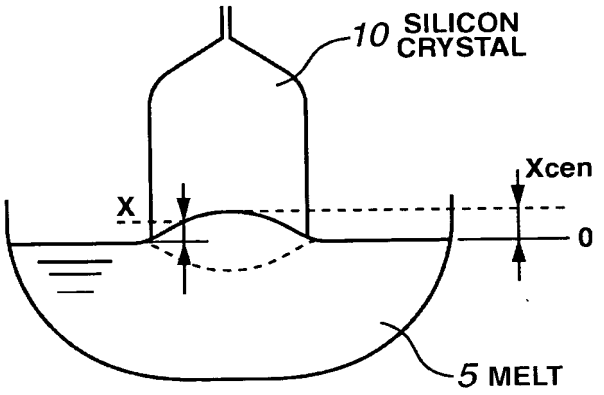

FIG.17

COMPARISON OF CONVENTIONAL COP REDUCTION METHOD AND PRESENT INVENTION

	REDUCTION IN COP COUNT OF AT LEAST 0.10 μm	PRODUCTIVITY	PRESENCE OR ABSENCE OF R-OSF
METHOD ①	△	◎	ABSENT
METHOD ②	○	△	PRESENT
METHOD ③	◎	△	ABSENT
PRESENT INVENTION	◎	○	ABSENT

◎: EXCELLENT, ○: GOOD, △: FAIR

FIG.18

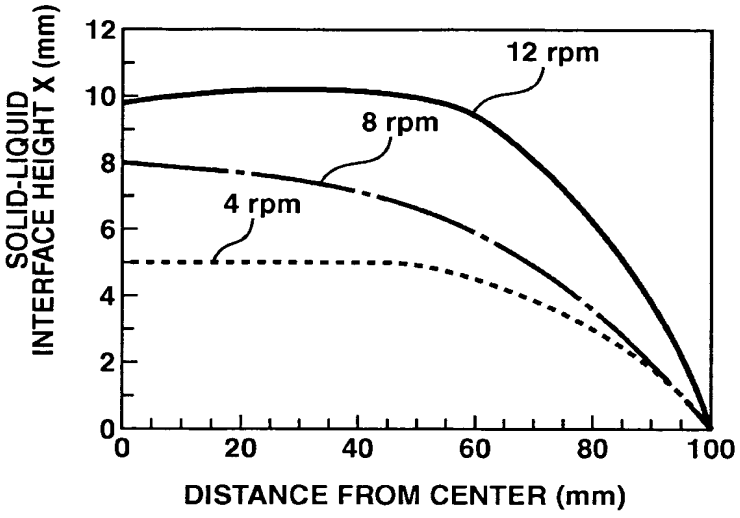

CHANGE IN SOLID-LIQUID INTERFACE SHAPE WHEN CRYSTAL ROTATION WAS VARIED (OTHER THAN CRYSTAL ROTATION, ALL PULLING CONDITIONS WERE THE SAME, NO MAGNETIC FIELD WAS APPLIED)

FIG.19

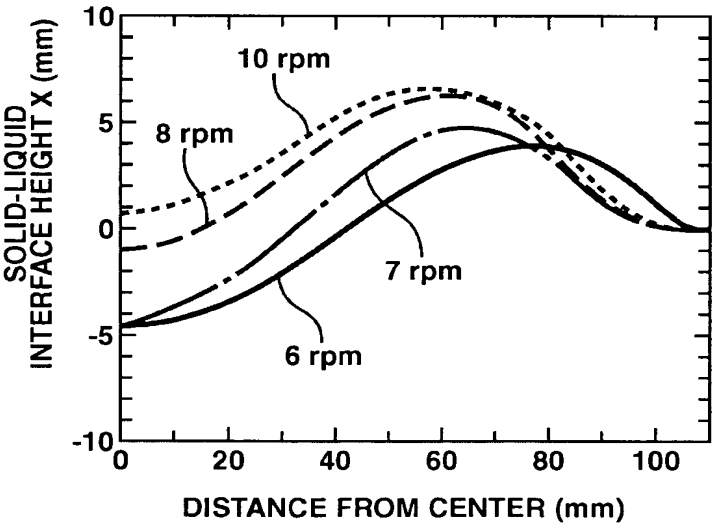

CHANGE IN SOLID-LIQUID INTERFACE SHAPE WHEN CRUCIBLE ROTATION WAS VARIED (OTHER THAN CRUCIBLE ROTATION, ALL PULLING CONDITIONS WERE THE SAME, NO MAGNETIC FIELD WAS APPLIED)

FIG.20

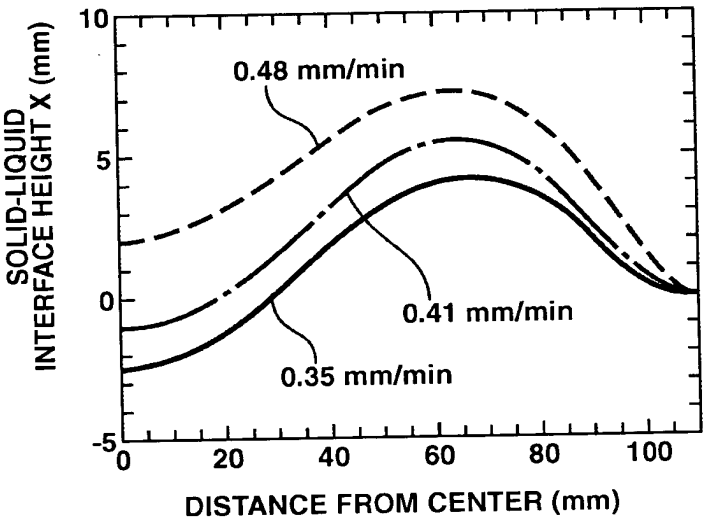

CHANGE IN SOLID-LIQUID INTERFACE SHAPE WHEN PULLING RATE WAS VARIED UNDER NORMAL PULLING CONDITIONS (NO MAGNETIC FIELD APPLIED, NO COOLER INSTALLED) (OTHER THAN PULLING RATE, ALL PULLING CONDITIONS WERE THE SAME)

FIG.21

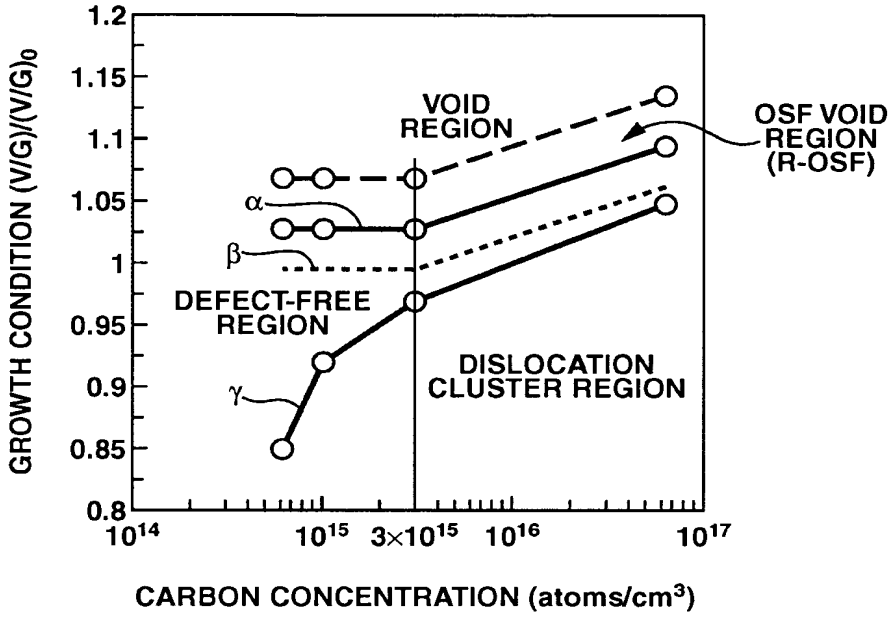
GROWTH CONDITION (V/G)/(V/G)0
1.2
1.15
1.1
1.05
1
0.95
0.9
0.85
0.8
VOID REGION
OSF VOID REGION (R-OSF)
α
β
γ
DEFECT-FREE REGION
DISLOCATION CLUSTER REGION
10^14
10^15
3×10^15
10^16
10^17
CARBON CONCENTRATION (atoms/cm3)

FIG.22

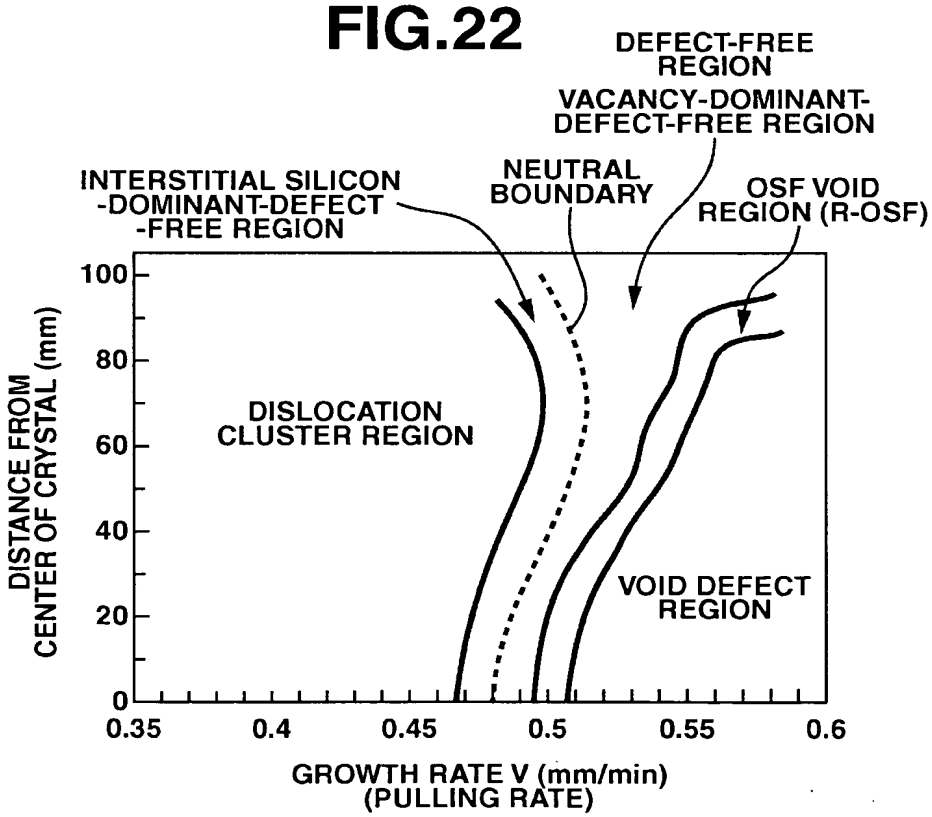
DEFECT-FREE REGION
VACANCY-DOMINANT-DEFECT-FREE REGION
INTERSTITIAL SILICON -DOMINANT-DEFECT -FREE REGION
NEUTRAL BOUNDARY
OSF VOID REGION (R-OSF)
DISTANCE FROM CENTER OF CRYSTAL (mm)
100
80
60
40
20
0
DISLOCATION CLUSTER REGION
VOID DEFECT REGION
0.35
0.4
0.45
0.5
0.55
0.6
GROWTH RATE V (mm/min) (PULLING RATE)

FIG.23

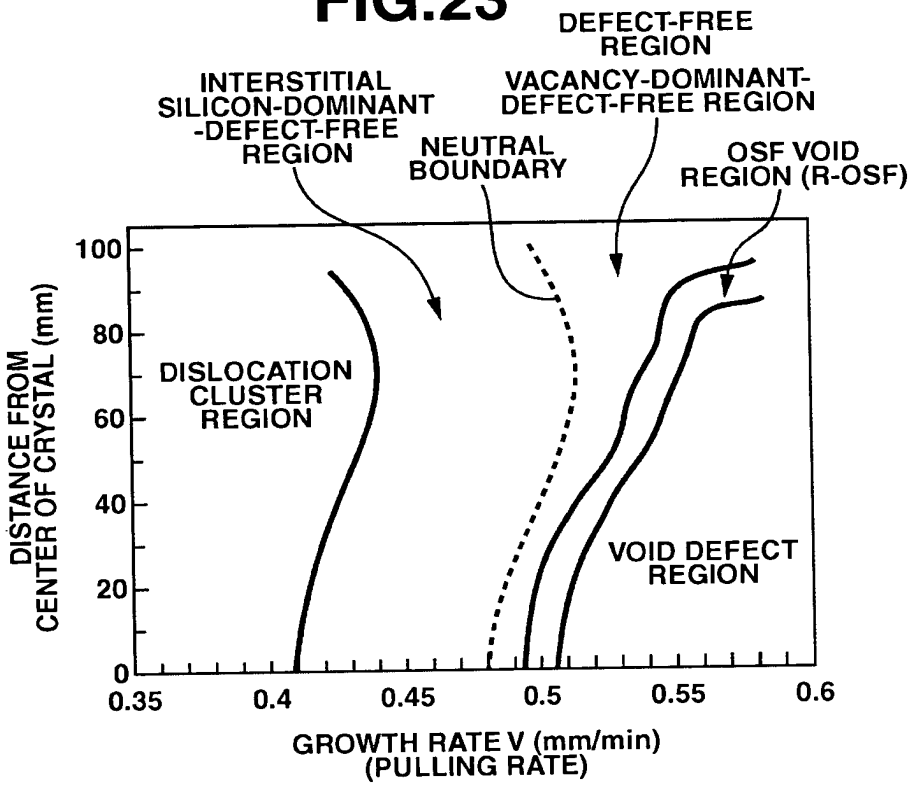

FIG.24

RELATIONSHIP BETWEEN CARBON CONCENTRATION AND $(V/G)/(V/G)_0$ AT THE BOUNDARY AT WHICH THE DEFECT TYPE CHANGES

CARBON CONCENTRATION (atoms/cm^3)	OSF BOUNDARY α (LOW V SIDE)	NEUTRAL POSITION β	DISLOCATION CLUSTER GENERATION BOUNDARY γ
6×10^{14}	1.03	1.00	0.85
1×10^{15}	1.03	1.00	0.92
3×10^{15}	1.03	1.00	0.97
6×10^{16}	1.095	1.07	1.05

FIG.25

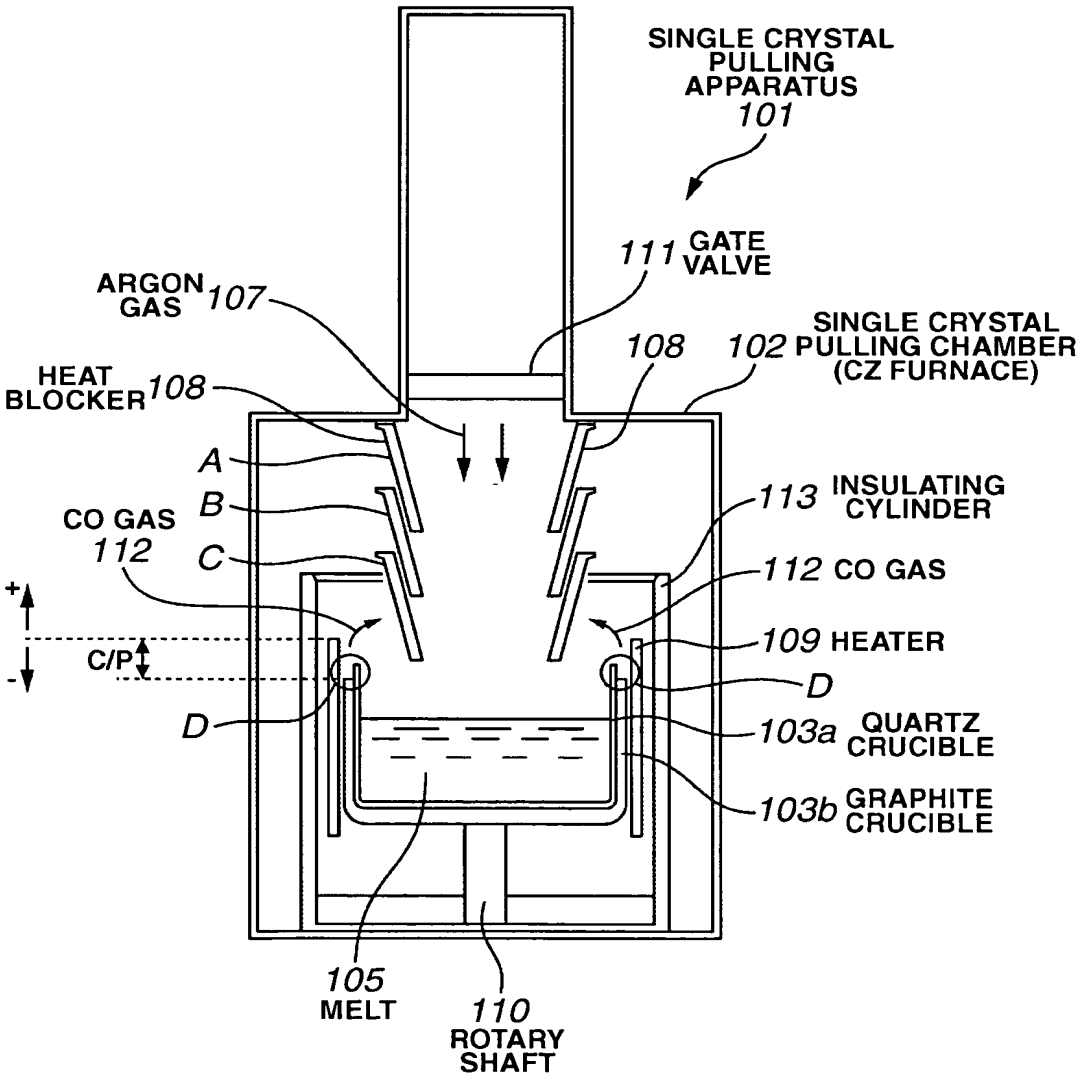
SINGLE CRYSTAL PULLING APPARATUS 101
111 GATE VALVE
ARGON GAS 107
108
102 SINGLE CRYSTAL PULLING CHAMBER (CZ FURNACE)
HEAT BLOCKER 108
A
B
C
CO GAS 112
113 INSULATING CYLINDER
112 CO GAS
+
C/P
-
109 HEATER
D
D
103a QUARTZ CRUCIBLE
103b GRAPHITE CRUCIBLE
105 MELT
110 ROTARY SHAFT

FIG.26

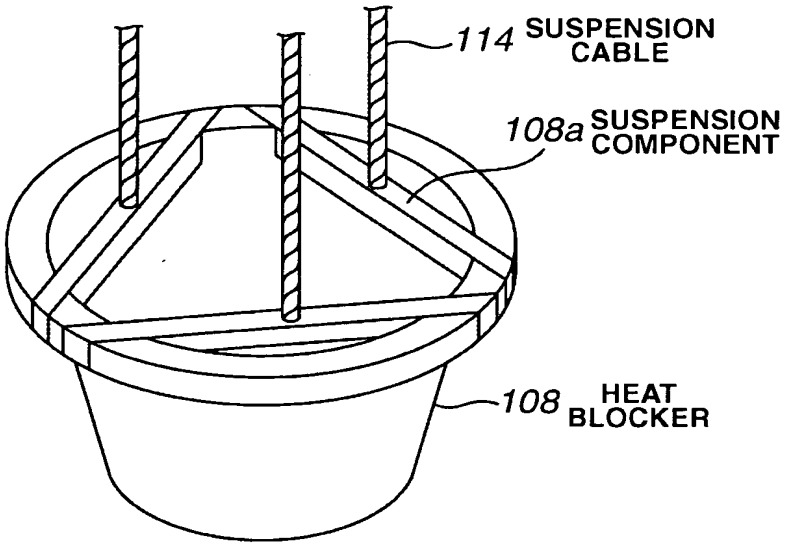
114 SUSPENSION CABLE
108a SUSPENSION COMPONENT
108 HEAT BLOCKER

FIG.27

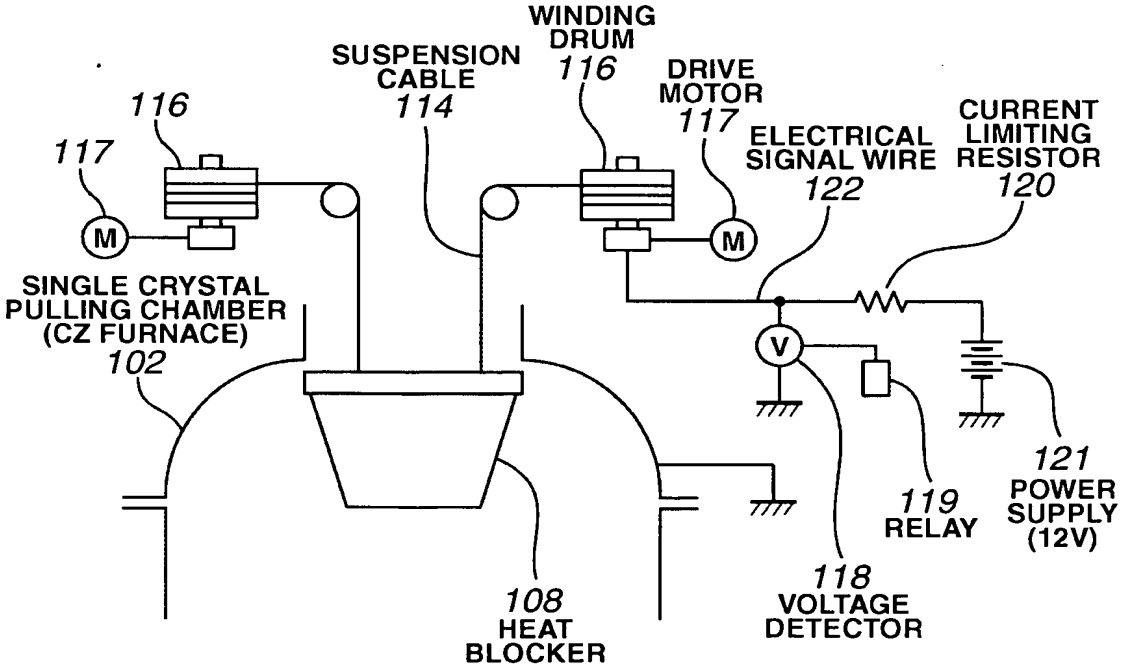
WINDING DRUM 116
SUSPENSION CABLE 114
DRIVE MOTOR 117
116
117
ELECTRICAL SIGNAL WIRE 122
CURRENT LIMITING RESISTOR 120
M
M
SINGLE CRYSTAL PULLING CHAMBER (CZ FURNACE) 102
V
121 POWER SUPPLY (12V)
119 RELAY
118 VOLTAGE DETECTOR
108 HEAT BLOCKER

FIG.28

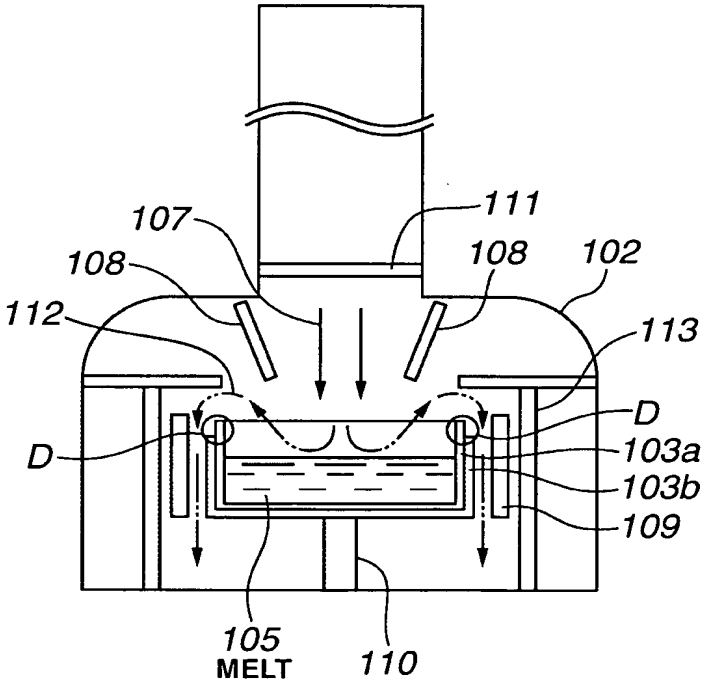

PRIOR ART **FIG.29**

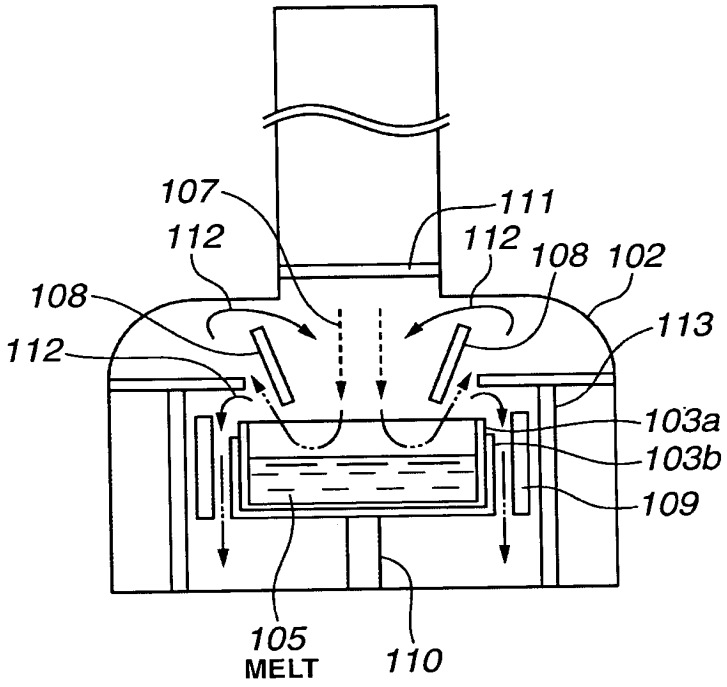

FIG.30

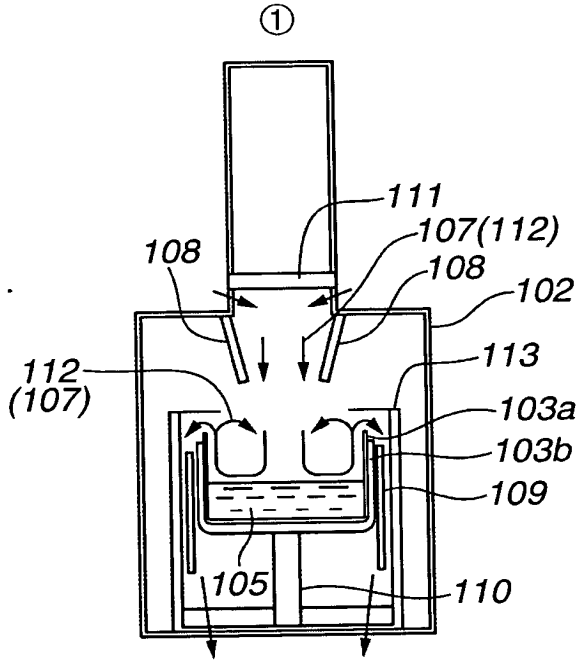

FIG.31

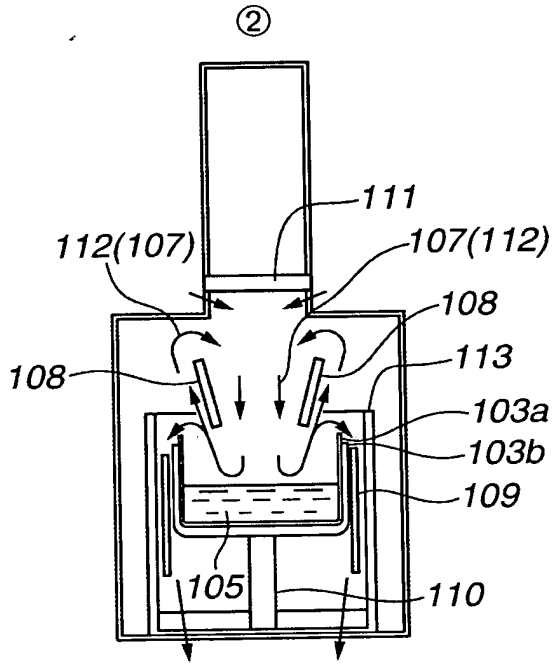
②
111
112(107)
107(112)
108
108
113
103a
103b
109
105
110

FIG.32

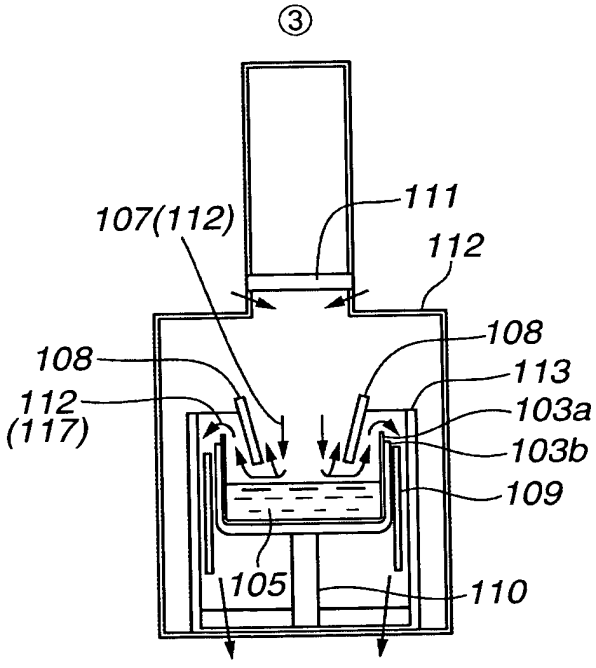
③
107(112)
111
112
108
108
113
112
(117)
103a
103b
109
105
110

FIG.33

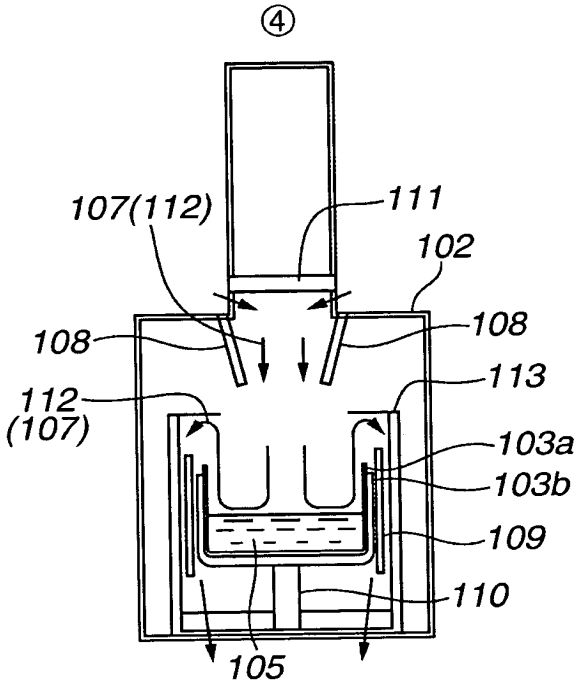
④
107(112)
111
102
108
108
113
112
(107)
103a
103b
109
110
105

FIG.34

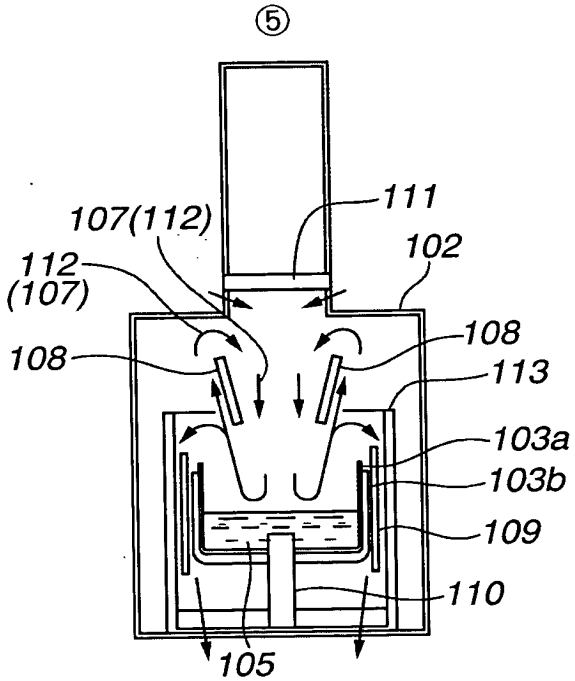
⑤
107(112)
111
102
112
(107)
108
108
113
103a
103b
109
110
105

FIG.35

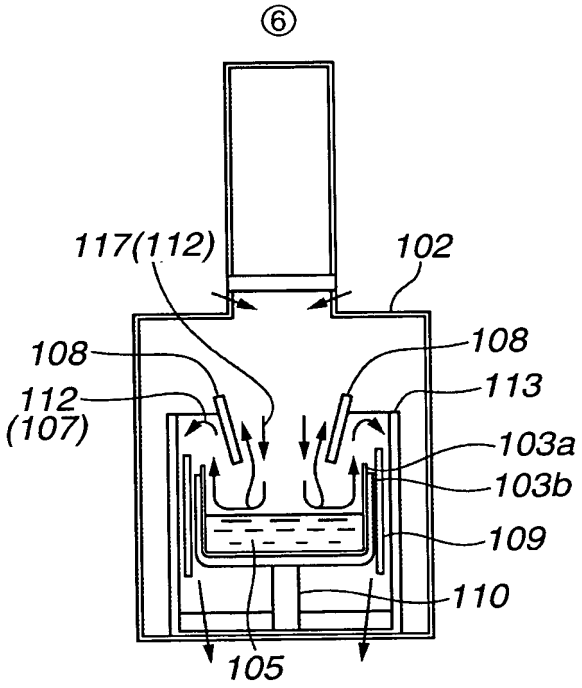

FIG.36

LEVEL	HEAT BLOCKER POSITION	CRUCIBLE POSITION C/P	CARBON CONCENTRATION RANKING (FROM LOWEST)
①	A	23	(2)
②	B	23	(6)
③	C	23	(4)
④	A	-100	(1)
⑤	B	-100	(5)
⑥	C	-100	(3)

FIG.37

CARBON CONCENTRATION (E17 atoms/cm^3)

CRUCIBLE POSITION C/P (mm) \ GAS FLOW (L/min)	80	120
30	0.08~0.09	0.08~0.09
-70		